JACC: CARDIOVASCULAR IMAGING VOL. 2, NO. 2, 2009

ISSN 1936-878X/09/$36.00
PUBLISHED BY ELSEVIER INC. DOI:10.1016/j.jcmg.2008.09.015

Characterization of Noncalcified Coronary Plaques and Identification of Culprit Lesions in Patients With Acute Coronary Syndrome by 64-Slice Computed Tomography

Toshiro Kitagawa, MD,* Hideya Yamamoto, MD, FACC,* Jun Horiguchi, MD,‡ Norihiko Ohhashi, MD,* Futoshi Tadehara, MD,* Tomoki Shokawa, MD,* Yoshihiro Dohi, MD,* Eiji Kunita, MD,* Hiroto Utsunomiya, MD,* Nobuoki Kohno, MD,† Yasuki Kihara, MD, FACC*

Hiroshima, Japan

OBJECTIVES We sought to characterize noncalcified coronary atherosclerotic plaques in culprit and remote coronary atherosclerotic lesions in patients with acute coronary syndrome (ACS) with 64-slice computed tomography (CT).

BACKGROUND Lower CT density, positive remodeling, and adjacent spotty coronary calcium are characteristic vessel changes in unstable coronary plaques.

METHODS Of 147 consecutive patients who underwent contrast-enhanced 64-slice CT examination for coronary artery visualization, 101 (ACS; n = 21, non-ACS; n = 80) having 228 noncalcified coronary atherosclerotic plaques (NCPs) were studied. Each NCP detected within the vessel wall was evaluated by determining minimum CT density, vascular remodeling index (RI), and morphology of adjacent calcium deposits.

RESULTS The CT visualized more NCPs in ACS patients (65 lesions, 3.1 ± 1.2/patient) than in non-ACS patients (163 lesions, 2.0 ± 1.1/patient). Minimum CT density (24 ± 22 vs. 42 ± 29 Hounsfield units [HU], $p < 0.01$), RI (1.14 ± 0.18 vs. 1.08 ± 0.19, $p = 0.02$), and frequency of adjacent spotty calcium of NCPs (60% vs. 38%, $p < 0.01$) were significantly different between ACS and non-ACS patients. Frequency of NCPs with minimum CT density <40 HU, RI >1.05, and adjacent spotty calcium was approximately 2-fold higher in the ACS group than in the non-ACS group (43% vs. 22%, $p < 0.01$). In the ACS group, only RI was significantly different between 21 culprit and 44 nonculprit lesions (1.26 ± 0.16 vs. 1.09 ± 0.17, $p < 0.01$), and a larger RI (≥1.23) was independently related to the culprit lesions (odds ratio: 12.3; 95% confidential interval: 2.9 to 68.7, $p < 0.01$), but there was a substantial overlap of the distribution of RI values in these 2 groups of lesions.

CONCLUSIONS Sixty-four-slice CT angiography demonstrates a higher prevalence of NCPs with vulnerable characteristics in patients with ACS as compared with stable clinical presentation. (J Am Coll Cardiol Img 2009;2:153–60) © 2009 by the American College of Cardiology Foundation

From the Departments of *Cardiovascular Medicine, and †Molecular and Internal Medicine, Graduate School of Biomedical Sciences, Hiroshima University, Hiroshima, Japan; and the ‡Department of Clinical Radiology, Hiroshima University Hospital, Hiroshima, Japan.

Manuscript received August 19, 2008; revised manuscript received September 16, 2008, accepted September 24, 2008.

JACC: CARDIOVASCULAR IMAGING, VOL. 2, NO. 2, 2009
FEBRUARY 2009:153–60

The recently developed technology of multidetector computed tomography (MDCT) has the potential to noninvasively identify and characterize noncalcified coronary atherosclerotic plaques (NCPs) in vivo (1,2). A potentially interesting application would be the identification of patients or individual coronary lesions with an increased likelihood of plaque rupture or erosion, leading to acute coronary events. Some previous studies have identified plaque characteristics typically observed by computed tomography (CT) in patients with acute coronary syndrome (ACS). Such characteristics included lower CT density, positive remodeling (PR), and adjacent spotty calcium deposits (3,4). We previously reported that, in comparison with intravascular ultrasound (IVUS), 64-slice CT allows reliable analysis of the components, vascular remodeling, and adjacent calcium morphology of NCPs and could document that lower CT density, PR, and adjacent spotty coronary calcium frequently co-existed in potentially "vulnerable" lesions (5). We consequently hypothesize that these morphologic factors of NCPs might act synergistically to increase the risk of ACS.

See page 161

Although most previous analyses were limited to culprit lesions in ACS patients (3,4), we designed the study reported here to characterize all NCPs—including nonculprit lesions—in patients with ACS with 64-slice CT. We also compared the NCP characteristics in patients with ACS with others with stable coronary artery disease.

ABBREVIATIONS AND ACRONYMS

ACS = acute coronary syndrome
CT = computed tomography
ECG = electrocardiogram
HU = Hounsfield units
IVUS = intravascular ultrasound
MDCT = multidetector computed tomography
NCP = noncalcified coronary atherosclerotic plaque
NSTEMI = non–ST-segment elevation myocardial infarction
PR = positive remodeling
RI = remodeling index

METHODS

Study patients. From November 2006 to October 2007, we enrolled 147 consecutive patients with proven or suspected coronary artery disease (96 men and 51 women, 67 ± 11 years), who underwent MDCT angiography for follow-up or diagnosis of coronary artery disease. Exclusion criteria for MDCT angiography included cardiac arrhythmias (i.e., atrial fibrillation or frequent paroxysmal premature beats), contraindications for iodinated contrast medium, unstable hemodynamic conditions, and ST-segment elevation myocardial infarction. Furthermore, patients with previous ACS, percutaneous coronary intervention, and/or coronary artery bypass grafting were excluded. The study was approved by our hospital's ethical committee, and written informed consent was obtained from all patients.

We assigned patients to the ACS (non–ST-segment elevation myocardial infarction [NSTEMI] and unstable angina) or the non-ACS group according to standard criteria (6). Specifically, NSTEMI was defined as a new finding of ST-segment depression of >0.1 mm or T-wave inversion of at least 0.3 mm in more than 2 anatomically contiguous leads and elevation of troponin-I levels (>0.05 ng/ml). Unstable angina was defined as a new onset of severe, progressive, or resting angina without elevation of electrocardiographic (ECG) ST-segment and troponin-I level. Patients without any of these criteria and with stable clinical presentation (equivocal or positive cardiac stress test, atypical chest pain, or stable exertional chest pain) were assigned to the non-ACS group.

For all patients in the ACS group, invasive coronary angiography was performed within 24 h after MDCT angiography. Vessel narrowing was measured with quantitative coronary angiography analysis (QCA-CMS, Version 5.3, MEDIS Medical Imaging Systems, Leiden, the Netherlands) in the projection that revealed the highest degree of stenosis, and obstructive stenosis was defined as luminal diameter narrowing >50% compared with the reference site. Per patient, 1 single obstructive coronary stenosis was identified as the culprit lesion. When multiple obstructive coronary stenoses were detected, the culprit lesion was defined as the lesion whose appearance was associated with ECG changes or as the lesion with the most obstructive luminal narrowing.

MDCT scan protocol and reconstruction. MDCT angiography was performed with a 64-slice CT scanner (LightSpeed VCT, GE Healthcare, Waukesha, Wisconsin; gantry rotation time, 0.35 s; 64 × 0.625 mm detector collimation, retrospective ECG gating). Patients with a resting heart rate ≥60 beats/min received 40 mg metoprolol orally 60 min before MDCT scanning; all received 0.3 mg nitroglycerin sublingually just before scanning. Our scan protocol and reconstruction methods have been described previously (5). In brief, after a plain scan to determine the calcium burden of the coronary tree and measure coronary calcium score according to the standard Agatston method (sequential scan with 16 × 2.5 mm collimation; tube current 140 mA; tube voltage 120 kV), we acquired a contrast-enhanced data set 30 to 50 ml (0.6 to 0.7 ml/kg) contrast medium (Iopamidol, 370 mg I/ml, Bayer Healthcare, Berlin, Germany) during an inspiratory

breath-hold. The volume data set was acquired in helical mode (64 × 0.625 mm collimation; CT pitch factor, 0.18 to 0.24:1; tube current, 600 to 750 mA with ECG-correlated tube current modulation; tube voltage, 120 kV). The effective radiation dose was estimated on the basis of the dose-length product and ranged from 15 to 18 mSv (5). Image reconstruction was performed with image-analysis software (CardIQ, GE Healthcare) on a dedicated computer workstation (Advantage Workstation Ver.4.2, GE Healthcare). A "standard" kernel was used as the reconstruction filter. Depending on heart rate, either a half-scan (temporal window = 175 ms) or multi-segment (temporal window <175 ms) reconstruction algorithm was selected, and the optimal cardiac phase with the least motion artifacts was chosen individually.

Evaluation of NCP characteristics. All coronary segments >2 mm in diameter were evaluated by 2 blinded and independent observers with curved multiplanar reconstructions and cross-sectional images rendered perpendicular to the vessel center line. The definitions of NCPs and coronary calcium were as follows (5): NCP: a low-density mass >1 mm^2 in size, located within the vessel wall and clearly distinguishable from the contrast-enhanced coronary lumen and the surrounding pericardial tissue; coronary calcium: a structure on the vessel wall with a CT density above that of the contrast-enhanced coronary lumen or with a CT density of >120 Hounsfield units (HU) assigned to the coronary artery wall in a plain image. For NCPs and calcium analyses, the optimal image display setting was chosen on an individual basis; in general, the window was between 700 and 1,000 HU, and the level between 100 and 200 HU.

As previously described (5), we determined the minimum CT density in each NCP by placing at least 5 regions of interest (area = 1 mm^2) in each lesion and documenting the lowest average value of all regions of interest, and on the basis of our previous results (5), low-density NCPs were defined as lesions with a minimum CT density of <40 HU. We also determined the extent of luminal enhancement of each coronary lesion by placing a region of interest (area = 1 mm^2) in the center of the coronary artery lumen at the respective reference segment. On the basis of measurements of the cross-sectional vessel areas (mm^2) at each NCP site of maximum vessel area and each proximal reference site of the same coronary artery, we calculated the "Remodeling Index" (RI). Positive remodeling was defined as RI >1.05 (7). Finally, we assessed calcium deposits in or adjacent to each NCP by determining their presence or absence and their morphology. Spotty calcium was defined as follows: length of calcium burden <3/2 of vessel diameter and width <2/3 of vessel diameter (8). If the initial classification of NCP and adjacent calcium differed among the 2 independent observers, final classification was achieved by consensus.

Statistical analysis. Coronary calcium score is expressed as median value and range, and other measurements are expressed as mean ± SD. Continuous and categorical variables were compared with the Mann-Whitney test and chi-square test, respectively. Interobserver variability of measured CT densities and cross-sectional vessel areas was determined by calculating Pearson's correlation coefficient. In comparisons between ACS and non-ACS lesions and culprit and nonculprit lesions, we used only lesion specific factors, not including patient characteristics because lesions clustered in a single patient. Parameters of NCPs were tested with a receiver-operator characteristic curve to assess their reliability as prognostic variables for predicting ACS culprit lesions. Logistic regression was used to examine the associations between NCP characteristics (RI, presence of adjacent spotty calcium, NCP CT density, and reference site CT density) and ACS culprit lesions for multivariate analysis adjusted for the location of NCPs. All analyses were done with JMP 5.0.1 statistical software (SAS Institute Inc., Cary, North Carolina). A p value of <0.05 was considered statistically significant.

RESULTS

Baseline characteristics. The mean heart rate during scanning was 61 ± 10 beats/min; mean scan time for coronary CT angiography was 6.3 ± 2.1 s. No patient experienced any complication due to MDCT, and no patient was excluded from analysis due to poor image quality of the 64-slice CT.

Of the 147 patients, 46 (31%) had no NCPs as detected by 64-slice CT angiography (31 patients had no coronary atherosclerotic lesions, and 15 patients had only calcified coronary lesions), and all 46 had presented with stable symptoms. In the remaining 101 patients (69%) (21 patients with ACS [8 NSTEMI and 13 unstable anginas] and 80 of 126 patients with stable clinical presentation [non-ACS: no symptom, atypical chest pain, or stable exertional chest pain]), CT angiography allowed detection of at least 1 coronary lesion that contained noncalcified components. A total of 228 NCPs were visualized (on average, 2.2 ± 1.2/patient; range, 1 to 5 lesions/patient). Clinical

JACC: CARDIOVASCULAR IMAGING, VOL. 2, NO. 2, 2009
FEBRUARY 2009:153–60

Table 1. Patients' Characteristics

	ACS Group (n = 21)	Non-ACS Group (n = 80)	p Value
Age (yrs)	66 ± 11	69 ± 9	NS
Male/female	17/4	61/19	NS
Hypertension	13 (62)	53 (66)	NS
Hyperlipidemia	12 (57)	37 (46)	NS
Diabetes mellitus	8 (38)	39 (49)	NS
Previous or current smoker	12 (57)	45 (56)	NS
Statin use	8 (38)	23 (29)	NS
Heart rate (beats/min)	59 ± 7	59 ± 9	NS
Body mass index (kg/m^2)	25 ± 3	24 ± 4	NS
Coronary calcium score	184 (0–1,550)	107 (0–4,656)	NS

N = 101. Coronary calcium score is expressed as median value (range). Other data are the mean value ± SD or n (%) of patients.
ACS = acute coronary syndrome.

characteristics of the 101 patients with NCPs are shown in Table 1. There were no statistically significant differences between ACS and non-ACS groups. Figure 1 shows MDCT and invasive angiographic findings in a case with ACS.

Comparisons of NCP findings between ACS and non-ACS patients. Sixty-five and 163 NCPs were detected in the ACS (n = 21) and non-ACS (n = 80) group, respectively. The location of NCPs in the ACS and non-ACS groups was similar (6% and 10% in the left main coronary artery, 37% and 39% in the left anterior descending artery, 20% and 15% in the left circumflex artery, 37% and 36% in the right coronary artery, respectively). The mean number of NCPs/patient was significantly higher in the ACS group (3.1 ± 1.2) than in the non-ACS group (2.0 ± 1.1, $p < 0.01$). Comparisons of NCP characteristics between the 2 groups are shown in Table 2. Excellent inter-observer agreement was found for minimum CT densities of NCPs (r = 0.91), for luminal densities at the reference site lumens (r = 0.94), and for all cross-sectional vessel areas (r = 0.88). The minimum CT density of NCPs was significantly lower in the ACS group (24 ± 22 HU) than in the non-ACS group (42 ± 29 HU, $p < 0.01$). There was no difference in mean CT densities of reference site lumens between the ACS and non-ACS groups. The mean RI of NCPs was significantly higher in the ACS group than in the non-ACS group (1.14 ± 0.18 vs. 1.08 ± 0.19, p = 0.02). Noncalcified coronary atherosclerotic plaques were more frequently associated with spotty calcification in the ACS group (60%) as compared with the non-ACS group (38%, $p < 0.01$). Furthermore, the frequency of low-density NCPs with PR and spotty calcium was substantially higher in the ACS group (43%) than in the non-ACS group (22%, $p < 0.01$).

CT characteristics of culprit versus nonculprit lesions in ACS patients. In the 21 ACS patients, 21 culprit and 44 nonculprit NCPs were detected. Of these lesions, 32 (21 culprit and 11 nonculprit) were assessed as obstructive (>50% stenosis) by invasive angiography. Comparisons of NCP characteristics between culprit and nonculprit lesions in the ACS group are shown in Table 3. The frequency of adjacent spotty calcium was similar in both types of plaques (57% vs. 61%). The minimum CT density of the culprit lesions tended to be lower than that of the nonculprit lesions (15 ± 13 HU vs. 28 ± 24 HU), but this difference did not reach statistical significance. The mean RI of the culprit lesions (1.26 ± 0.16) was significantly higher than that of the nonculprit lesions (1.09 ± 0.17, $p < 0.01$), but there was a substantial overlap of the distribution of RI values in these 2 groups of lesions (Fig. 2). The optimal cutoff for RI by CT angiography to predict culprit lesions was 1.23 and had a sensitivity of 71% and specificity of 82% (area under the curve 0.77). The frequency of plaques that displayed all 3 parameters of "vulnerability" (low CT density, positive remodeling, and spotty calcium) tended to be higher for culprit lesions (57%) compared with nonculprit lesions (36%). However, the difference was not significant. Multivariate analysis, which included larger RI (≥1.23), the presence of adjacent spotty calcium, the minimum NCP CT density, and the reference site CT density, revealed that a larger RI was the only significant predictor of ACS culprit lesions (odds ratio: 12.3; 95% confidence interval: 2.9 to 68.7, $p < 0.01$). Furthermore, the mean RI of the 21 culprit lesions was significantly higher than that of the 11 obstructive nonculprit lesions (1.26 ± 0.16 vs. 1.08 ± 0.16, $p < 0.01$), whereas the minimum CT densities (15 ± 13 HU vs. 15 ± 18 HU), frequencies of adjacent spotty calcium (57% vs. 64%), and frequencies of low-density NCPs with PR and spotty calcium (57% vs. 45%) were similar.

DISCUSSION

In this study, we demonstrated that 64-slice CT coronary angiography allows visualization of more noncalcified coronary atherosclerotic lesions with characteristics assumed to be associated with plaque "vulnerability" in patients with ACS as compared with patients with stable clinical presentation. Thus, 64-slice CT might contribute toward the differentiation of "vulnerable patients." Furthermore, we observed that a high degree of positive remodeling is the most

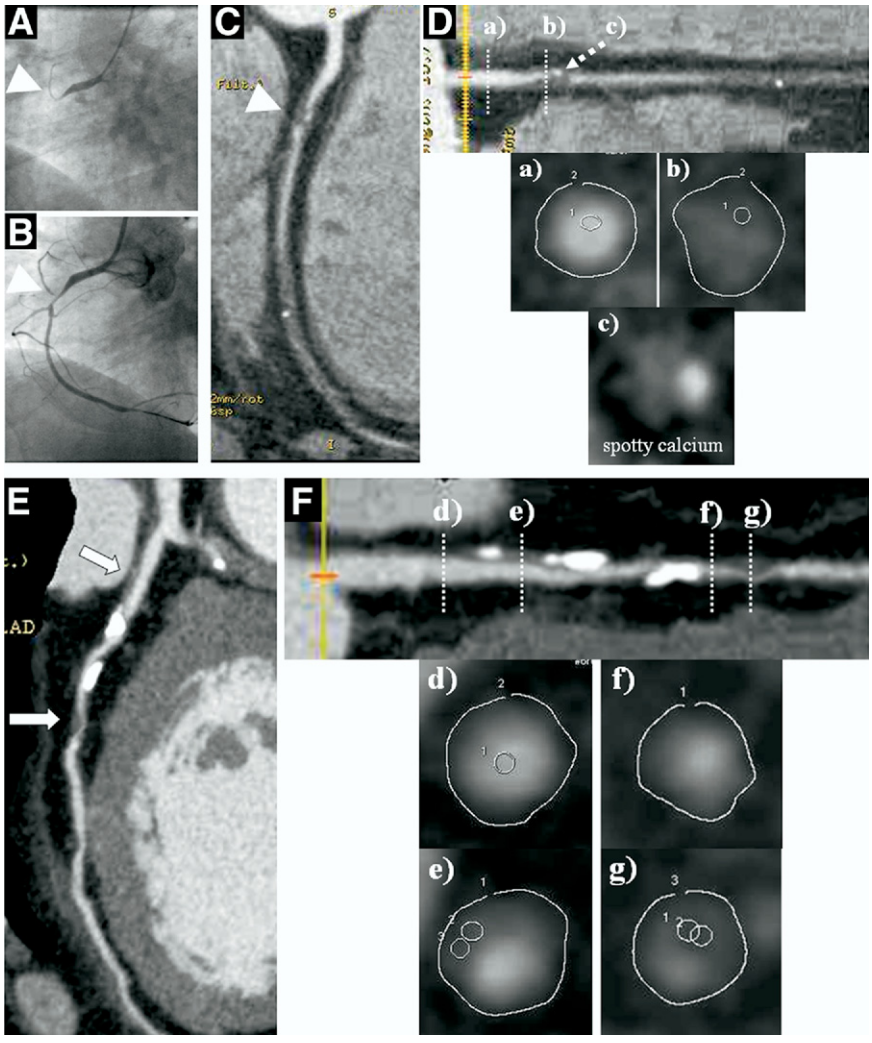

Figure 1. Invasive Angiography and Coronary CT Angiography in a 58-Year-Old Man With NSTEMI

(A and B) Invasive coronary angiographic images show an initial occlusion of the proximal portion of the right coronary artery (RCA) **(arrowhead)** and a recanalization of the lesion. **(C** and **D)** Curved multiplanar reconstruction (MPR) images show the subtotal occlusion and noncalcified coronary atherosclerotic plaque (NCP) with spotty calcium in the proximal portion of the RCA **(arrowhead)**. The cross-sectional vessel areas of the reference site **(a)** and NCP **(b)** are 23 and 29 mm^2, respectively. Therefore, the remodeling index (RI) is 1.26. The minimum computed tomography (CT) density of the NCP is 16 Hounsfield units (HU) **(b)**. Spotty calcium with the NCP is observed in the cross-sectional image **(c)**. **(E and F)** Curved MPR images show multiple nonculprit NCP in left anterior descending coronary artery (LAD) **(arrows)**. The cross-sectional vessel areas of the reference site **(d)** and nonobstructive NCP **(e)** in the proximal portion are 28 and 28 mm^2, respectively. Therefore, the RI is 1.0. The minimum CT density of the NCP is 44 HU **(e)**. The cross-sectional vessel areas of the reference site **(f)** and obstructive NCP **(g)** in the middle portion are 18 and 18 mm^2, respectively. Therefore, the RI is 1.0. The minimum CT density of the NCP is −7 HU **(g)**. NSTEMI = non–ST-segment elevation myocardial infarction.

accurate discriminator of culprit and nonculprit lesions in ACS patients. Thus, our results provide further evidence for the potential of MDCT angiography to noninvasively identify vulnerable lesions and vulnerable patients.

General findings of NCPs in ACS. In a report using 16-slice CT angiography, the prevalence of noncalcified plaque was 100% in ACS culprit lesions (3). The present study on 64-slice CT also confirms the presence of NCPs in all ACS patients and in all ACS culprit lesions, whereas no patient without any NCP had an ACS. Although the number of ACS patients was small (n = 21), this indicates a high sensitivity of NCP as detected by CT to identify patients with ACS.

Furthermore, our findings are in accordance with previous evidence that the disease process in ACS patients is not focal but more widespread throughout

JACC: CARDIOVASCULAR IMAGING, VOL. 2, NO. 2, 2009
FEBRUARY 2009:153–60

Table 2. Comparison of NCP Characteristics Between ACS and Non-ACS Groups

	ACS Group (n = 65)	Non-ACS Group (n = 163)	p Value
CT density (HU)			
NCPs (minimum density)	24 ± 22	42 ± 29	< 0.01
Reference site	351 ± 44	357 ± 62	0.46
Remodeling index	1.14 ± 0.18	1.08 ± 0.19	0.02
Adjacent spotty calcium, (n [%])	39 (60)	62 (38)	< 0.01
Low-density NCPs (<40 HU) with PR and spotty calcium, (n [%])	28 (43)	36 (22)	< 0.01

Data are the mean value ± SD or n (%) of non-calcified coronary atherosclerotic plaque (NCPs).
ACS = acute coronary syndrome; CT = computed tomography; HU = Hounsfield units; PR = positive remodeling.

the coronary circulation and might lead to instability of multiple plaques (9). In fact, multiple plaque ruptures in locations other than on the culprit lesion have been detected by IVUS in patients with ACS (10). In the present study, with 64-slice CT angiography that can evaluate the entire coronary tree, more NCPs/patient were detected in the ACS group than the non-ACS group, and those that were detected more frequently displayed "vulnerable" characteristics, such as lower CT density, extent of arterial remodeling, and presence of adjacent spotty calcium. Motoyama et al. (4) reported that 47% of culprit lesions in ACS had all 3 characteristics of PR (RI >1.1), low CT density (<30 HU), and spotty calcium (<3 mm in size). We also observed that 43% of NCPs in the ACS group had all 3 vulnerable characteristics, although the criteria we used varied slightly. This indicates that multiple vulnerable plaques with characteristics similar to the culprit lesion are often present in the entire coronary tree of ACS patients.

Predictors of ACS culprit lesions in MDCT. A previous study with CT angiography (4) revealed that, among the 3 vulnerable characteristics, positive remodeling was the strongest discriminator between culprit and nonculprit lesions in patients with ACS (PR: 87%; low CT density: 79%; spotty calcium: 63%), similar to our results. Whereas this could be explained by previous data, such as a histopathological study using postmortem hearts that revealed that coronary plaques with PR had a higher lipid content and a higher macrophage count (11), or the fact that excessive expansive remodeling promotes continued local lipid accumulation, inflammation, oxidative stress, matrix breakdown, and eventually further plaque progression (12), this observation has to be interpreted with caution. In a retrospective analysis such as ours, the correlation of remodeling and culprit lesions might be a consequence of plaque rupture and not necessarily a predictor. Also, in spite of a significant difference of the mean RI between culprit and nonculprit lesions of ACS patients, the overlap of RI values in these 2 groups was substantial.

Study limitations. Caution is required when interpreting CT densities of NCPs. We cannot exclude the possibility that thrombosis might be present in some ACS culprit lesions, and low-density NCPs are indistinguishable from thromboses due to their similar densities. Thrombosis adjacent to very-low-density NCPs might increase the CT densities that were measured, and this might be 1 of the reasons that the minimum CT density is not statistically different between the culprit and nonculprit lesions in the present study. We believe that selecting the minimum density value as the NCP density is an appropriate method for limiting partial volume and beam hardening effects resulting from neighboring structures, especially hyperdense calcium. However, improvements of spatial resolution will be necessary to more reliably identify and characterize NCPs on the basis of CT densities.

Second, at present, there is no gold standard for determination of coronary plaque vulnerability in CT angiography. For example, in the previous MDCT study, spotty calcium was defined as <3 mm in size (4). However, the visual estimation of high-density structures, such as calcium deposits, varies depending on the window setting in the CT image. Therefore, we believe that our method, which is based on the comparison of calcium dimensions with vessel diameters, is more appropriate for classification of calcium deposits.

Table 3. Comparison of NCP Characteristics Between Culprit and Non-Culprit Lesions in ACS Group

	Culprit Lesions (n = 21)	Non-Culprit Lesions (n = 44)	p Value
CT density (HU)			
NCPs (minimum density)	15 ± 13	28 ± 24	0.07
Reference site	353 ± 46	350 ± 43	0.95
Remodeling index	1.26 ± 0.16	1.09 ± 0.17	< 0.01
Adjacent spotty calcium, (n [%])	12 (57)	27 (61)	0.75
Low-density NCPs (<40 HU) with PR and spotty calcium, (n [%])	12 (57)	16 (36)	0.11

Data are the mean value ± SD or n (%) of NCPs.
Abbreviations as Table 2.

Third, the present study is retrospectively designed, and we assume that vulnerable NCPs have morphological characteristics similar to those of already-disrupted NCPs—a limitation shared with previous studies in this field. A long-term, large prospective trial would be necessary to determine whether CT stratification of NCPs indeed has prognostic value for predicting future cardiac events. Future approaches might, in fact, extend beyond CT analysis of plaque morphology, such as demonstrated by a recent report that described the use of a dedicated contrast agent to visualize macrophage infiltration in atherosclerotic plaques (13).

Finally, our data acquisition protocol led to a relatively high radiation dose for coronary CT angiography. Recently, a prospectively ECG-triggered algorithm has been developed that allows imaging with substantially reduced dose (14). Further studies will be required to validate the accuracy for identification and characterization of NCPs with newer low-dose algorithms.

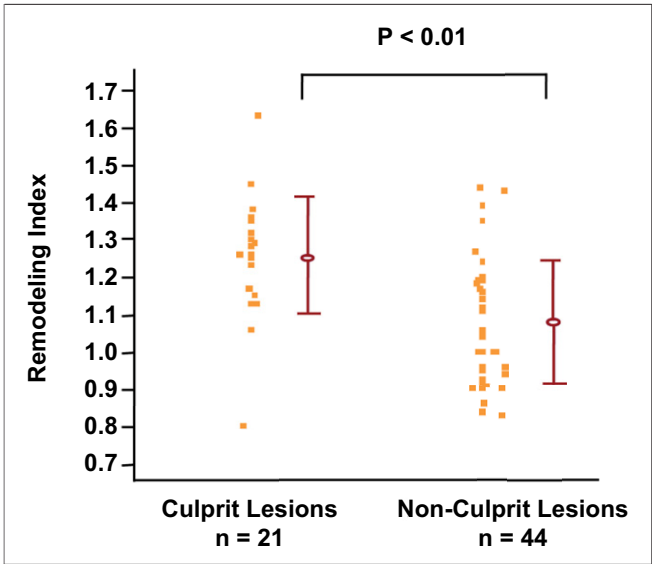

Figure 2. Comparison of RI Between ACS Culprit and Nonculprit Lesions

The mean RI of the culprit lesions is significantly higher than that of the non-culprit lesions (1.26 ± 0.16 vs. 1.09 ± 0.17, $p < 0.01$), but there is a substantial overlap of the distribution of RI values in these 2 groups of lesions. ACS = acute coronary syndrome; RI = remodeling index.

CONCLUSIONS

We were able to demonstrate that 64-slice coronary CT angiography detects a higher number of atherosclerotic lesions with noncalcified components in patients with ACS as compared with patients with stable symptoms. Identifying the actual culprit lesion in ACS patients is more difficult: among the characteristics that are assumed to be associated with plaque "vulnerability" in CT, a large degree of positive remodeling was the only independent predictor of culprit lesions in ACS patients, but a large variability was observed concerning the extent of positive remodeling in culprit and nonculprit lesions. Rather than identifying a single lesion responsible for a future coronary event, the ability to investigate plaque characteristics throughout the entire coronary system in a noninvasive fashion might be an important property of coronary CT angiography regarding its potential application in the context of identifying "vulnerable patients" at risk for ACS.

Acknowledgments

The authors are grateful to Nobuhiko Hirai, MD, and Masao Kiguchi, RT, for their technical assistance. The authors also thank Dr. Shozo Miki for his critical reading of the manuscript.

Reprint requests and correspondence: Dr. Hideya Yamamoto, Department of Cardiovascular Medicine, Graduate School of Biomedical Sciences, Hiroshima University, 1-2-3 Kasumi Minami-ku, Hiroshima 734-8551, Japan. *E-mail: hideyayama@hiroshima-u.ac.jp.*

REFERENCES

1. Hausleiter J, Meyer T, Hadamitzky M, et al. Prevalence of noncalcified coronary plaques by 64-slice computed tomography in patients with an intermediate risk for significant coronary artery disease. J Am Coll Cardiol 2006;46:312–8.
2. Butler J, Shapiro M, Reiber J, et al. Extent and distribution of coronary artery disease: A comparative study of invasive versus noninvasive angiography with computed tomography. Am Heart J 2007;153:378–84.
3. Hoffmann U, Moselewski F, Nieman K, et al. Noninvasive assessment of plaque morphology and composition in culprit and stable lesions in acute coronary syndrome and stable lesions in stable angina by multidetector computed tomography. J Am Coll Cardiol 2006;47:1655–62.
4. Motoyama S, Kondo T, Sarai M, et al. Multislice computed tomographic characteristics of coronary lesions in acute coronary syndromes. J Am Coll Cardiol 2007;50:319–26.
5. Kitagawa T, Yamamoto H, Ohhashi N, et al. Comprehensive evaluation of noncalcified coronary plaque characteristics detected using 64-slice computed tomography in patients with proven or suspected coronary artery disease. Am Heart J 2007;154:1191–8.
6. Braunwald E, Antman EM, Beasley JW, et al. ACC/AHA 2002 guideline update for the management of patients with unstable angina and non–ST-segment elevation myocardial infarction-summary article: a report of the American College of Cardiology/American Heart Association Task Force on Practice Guidelines (Committee on the Management of Patients With Unstable Angina). J Am Coll Cardiol 2002;40:1366–74.

JACC: CARDIOVASCULAR IMAGING, VOL. 2, NO. 2, 2009
FEBRUARY 2009:153–60

7. Achenbach S, Ropers D, Hoffmann U, et al. Assessment of coronary remodeling in stenotic and nonstenotic coronary atherosclerotic lesions by multidetector spiral computed tomography. J Am Coll Cardiol 2004;43:842–7.
8. Kajinami K, Seki H, Takekoshi N, et al. Coronary calcification and coronary atherosclerosis: site by site comparative morphologic study of electron beam computed tomography and coronary angiography. J Am Coll Cardiol 1997;29:1549–56.
9. Buffon A, Biasucci LM, Liuzzo G, et al. Widespread coronary inflammation in unstable angina. N Eng J Med 2002;347:5–12.
10. Rioufol G, Finet G, Ginon I, et al. Multiple atherosclerotic plaque rupture in acute coronary syndrome: a three-vessel intravascular ultrasound study. Circulation 2002;106:804–8.
11. Varnava AM, Mills PG, Davies MJ. Relationship between coronary artery remodeling and plaque vulnerability. Circulation 2002;105:939–43.
12. Chatzizisis YS, Coskun AU, Jonas M, Edelman ER, Feldman CL, Stone PH. Role of endothelial shear stress in the natural history of coronary atherosclerosis and vascular remodeling: molecular, cellular, and vascular behavior. J Am Coll Cardiol 2007;49:2379–93.
13. Hyafil F, Cornily JC, Feig JE, et al. Noninvasive detection of macrophages using a nanoparticulate contrast agent for computed tomography. Nat Med 2007;13:636–41.
14. Earls JP, Berman EL, Urban BA, et al. Prospectively gated transverse coronary CT angiography versus retrospectively gated helical technique: improved image quality and reduced radiation dose. Radiology 2008;246:742–53.

Key Words: acute coronary syndrome ■ multidetector computed tomography ■ noncalcified coronary plaque.